Fermi National Accelerator Laboratory

FERMILAB-FN-648

The Quasi-Isochronous Buckets of the Muon Collider

King-Yuen Ng

Fermi National Accelerator Laboratory
P.O. Box 500, Batavia, Illinois 60510

August 1996

Operated by Universities Research Association Inc. under Contract No. DE-AC02-76CHO3000 with the United States Department of Energy

Disclaimer

Distribution

FN-648

The Quasi-Isochronous Buckets of the Muon Collider

King-Yuen Ng

Fermi National Accelerator Laboratory, P.O. Box 500, Batavia, IL 60510*

(August 1996)

Abstract

In order to maintain a reasonable rf system, it is necessary for the muon collider to have a slippage factor $\eta < 1 \times 10^{-6}$ for all the particles in the bunch. The buckets dominated by the zeroth order, first order, or second order of η are examined, and the required rf voltages are computed. The problem of microwave instability is addressed. The reliability of computing higher-order momentum-compaction factor using a lattice code is discussed.

Expanded from a talk given at the
2+2 TeV $\mu^+\mu^-$ Collider Collaboration Meeting
at Fermilab, April 1-3, 1996

*Operated by the Universities Research Association, Inc., under contract with the U.S. Department of Energy.

I. INTRODUCTION

The high luminosity of the recently proposed 2 TeV-2 TeV muon-muon collider calls for a collider ring of circumference $C_0 = 2\pi R \sim 8000$ m with an rms bunch length of $\sigma_\ell = 3$ mm (10 ps) and rms momentum spread of $\sigma_\delta = 0.15\%$. The short bunch length as well as a reasonable rf voltage limit the slippage factor of the collider to $\eta \lesssim 1 \times 10^{-6}$, which is to be discussed in Sec. II. Section III reveals the disadvantages of the α-like bucket one would expect when the ring is operated so close to being isochronous. In Sec. IV, sextupoles are inserted into the arc regions to eliminate the first order of the momentum-compaction factor in momentum offset. This restores the bucket to pendulum-like. There is a choice of making the lattice second order or zeroth order momentum-compaction dominant. These two situations are discussed in Sec. V and Sec. VI. The reliability of computing the second-order momentum-compaction using lattice codes is addressed in Sec. VII. The problem of microwave instability of the muon bunches in a ring operated so near to transition is discussed in Sec. VIII. Finally, conclusions are given in Sec. IX.

II. LIMITATION OF SLIPPAGE FACTOR

When a muon bunch is delivered to the muon collider ring from the accelerator, it may be lengthened or shortened due to the potential distortion of the rf force. Besides this, however, the bunch can also be lengthened due to the excessive debunching $\Delta\ell$ between two consecutive passages through the rf system. Since the rf system is most likely concentration in one location of the ring, we must have

$$\Delta\ell = |\eta| C_0 \sigma_\delta \ll \sigma_\ell \ , \tag{2.1}$$

with C_0 denoting the length of the on-momentum closed orbit, or

$$|\eta| \ll \frac{\sigma_\ell}{\sigma_\delta C_0} \ll 2.5 \times 10^{-4} \ . \tag{2.2}$$

The above is only the limitation set by the lattice of the ring. For debunching in one turn, the rf system must supply enough energy to place the debunched particle back into the bunch. This amount of energy is given by

$$\Delta E = \frac{eVh\Delta\ell}{R} \ , \tag{2.3}$$

where h the rf harmonic, V the rf voltage, and $E = 2$ TeV the energy of the muons. Substituting $\sigma_\delta E$ and σ_ℓ for ΔE and $\Delta\ell$, respectively, Eq. (2.2) gives $hV = 1.273 \times 10^6$ GV. With $h = 6.667 \times 10^4$ so that the bucket width is about 40 times the rms bunch length, we arrive at $V = 19.10$ GV, which is certainly too large to achieve. For this reason, the slippage factor must be made very much less than 2.5×10^{-4}, and its limitation must be discussed together with the rf voltage.

For a small bunch, the bunch length and momentum spread are related by

$$\nu_s \sigma_\ell = R|\eta|\sigma_\delta \ , \tag{2.4}$$

where the synchrotron tune is given by

$$\nu_s = \sqrt{\frac{h|\eta|eV}{2\pi\beta^2 E}} \ . \tag{2.5}$$

Putting in numbers, we arrive at

$$\frac{hV}{|\eta|} = 5.093 \times 10^{12} \text{ MV} \ . \tag{2.6}$$

Let k denotes the ratio of total bucket length to rms bunch length. We can then compute the rf voltage for $|\eta| = 1 \times 10^{-5}$ and 1×10^{-6}, and the results are listed in Table I. The total length of a bunch is usually 5 to 6 times its rms values, so that 40 to 80 is a reasonable value for k. We can see from the table that for a reasonable rf voltage, we must restrict the slippage factor to $|\eta| \lesssim 1 \times 10^{-6}$ for all muons in the bunch, where $|\delta| < \delta_{\max} \approx 2\sigma_\delta$.

When the slippage factor is small enough, the next order may become important. The closed-orbit length C at momentum offset δ can be expanded as

$$C = C_0(1 + \alpha_0\delta + \alpha_1\delta^2 + \alpha_2\delta^3 + \cdots) \ , \tag{2.7}$$

where α_0 is the lowest order of the momentum-compaction factor of the lattice and $\alpha_1, \alpha_2, \cdots$ are the higher orders. On the other hand, we want the phase-slip equation to be written as

$$\frac{d\Delta\phi}{dt} = \omega_0\eta\delta \ , \tag{2.8}$$

where the definition of the slippage factor

$$\frac{\Delta T}{T_0} = \eta\delta = \eta_0\delta + \eta_1\delta^2 + \eta_2\delta^3 + \cdots \ , \tag{2.9}$$

Table I: RF voltages corresponding to different slippage factors and rf harmonics.

k	h	$\lvert\eta\rvert$	V (MV)	ν_s
20	1.333×10^5	1×10^{-5}	383.0	6.37×10^{-3}
		1×10^{-6}	38.3	6.37×10^{-4}
40	6.667×10^4	1×10^{-5}	763.9	6.37×10^{-3}
		1×10^{-6}	76.4	6.37×10^{-4}
80	3.333×10^4	1×10^{-5}	1528	6.37×10^{-3}
		1×10^{-6}	153	6.37×10^{-4}

has been used. In the above, $\omega_0/2\pi$ is the revolution frequency of the on-momentum particle. The detail is derived in the Appendix. Since the revolution period T is equal to orbit length divided by velocity, it is then not difficult to obtain

$$\eta_0 = \alpha_0 - \frac{1}{\gamma^2} \ , \tag{2.10}$$

$$\eta_1 = \alpha_1 + \frac{3\beta^2}{2\gamma^2} - \frac{\eta_0}{\gamma^2} \ , \tag{2.11}$$

$$\eta_2 = \alpha_2 + \frac{\alpha_1}{\gamma^2} - \frac{2\beta^4}{\gamma^2} + \frac{3\alpha_0\beta^2}{2\gamma^2} + \frac{\eta_0}{\gamma^4} \ , \tag{2.12}$$

where γ and β are the relativistic Lorentz factors of the on-momentum particle. For a 2 TeV muon, $\gamma^{-2} = 2.73 \times 10^{-9}$ which is very much less than the required $|\eta|$. Therefore, we have rather accurately, $\eta_1 \approx \alpha_1$ and $\eta_2 \approx \alpha_2$.

III. THE η_0 and η_1-DOMINATED ASYMMETRIC BUCKET

When $\eta_0 \lesssim 1 \times 10^{-6}$, we need to include the next lowest nonlinear term of the slippage factor. The Hamiltonian describing the motion of particle in the longitudinal phase space becomes

$$H = \left(\frac{\eta_0 \delta^2}{2} + \frac{\eta_1 \delta^3}{3} \right) h\omega_0 + \frac{eV\omega_0}{2\pi\beta^2 E} \left[\cos(\phi_s + \Delta\phi) + \Delta\phi \sin\phi_s \right] \ , \tag{3.1}$$

where ϕ_s is the synchronous phase. With the presence of η_1, the symmetry of the higher- and lower-momentum parts of the phase space is broken. As a

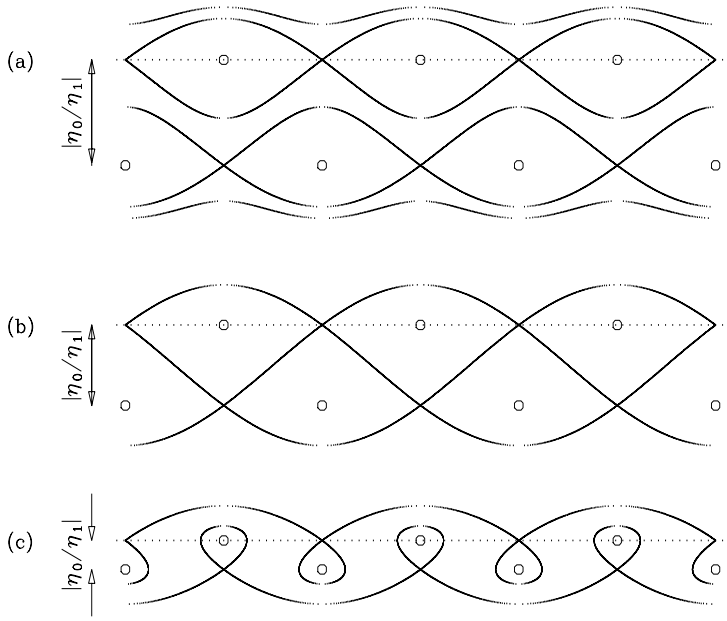

Figure 1: (a) When $|\eta_0/\eta_1|$ is not too small, the longitudinal phase space shows 2 series of distorted pendulum-like buckets. (b) As $|\eta_0/\eta_1|$ decreases to the critical value in Eq. (3.2), the 2 series merge. (c) Further reduction of $|\eta_0/\eta_1|$ leads to new pairing of stable and unstable fixed points and the buckets become α-like. In each case, the dotted line is the phase axis at zero momentum spread, and the small circles are the stable fixed points.

result, the phase-space structure will be very much disturbed. This Hamiltonian gives stable fixed points at $(2n\pi, 0)$, $(2(n+1)\pi - 2\phi_s, -\eta_0/\eta_1)$ and unstable fixed points at $(\ 2(n+1)\pi - 2\phi_s, 0)$, $(2n\pi, -\eta_0/\eta_1)$, where n is any integer. When the contribution of η_1 is much smaller than that of η_0, the buckets are still roughly pendulum-like as shown in Fig. 1(a) for the case of $\phi_s = 0$. Note that there is another series of buckets at momentum spread $-\eta_0/\eta_1$. As $|\eta_0/\eta_1|$ decreases to a point when the values of the Hamiltonian through all unstable fixed points are equal, the two series merge as shown in Fig. 1(b). This happens when

$$\left|\frac{\eta_0}{\eta_1}\right| = \left\{\frac{6eV}{\pi\beta^2 h\eta_0 E}\left[\left(\frac{\pi}{2} - \phi_s\right)\sin\phi_s - \cos\phi_s\right]\right\}^{1/2} . \tag{3.2}$$

The right-hand side is just $\sqrt{3}$ times the half bucket height when the η_1

term in the Hamiltonian is absent. As $|\eta_0/\eta_1|$ is further reduced, the pairing of the stable and unstable fixed points is altered, and the bucket become α-like as illustrated in Fig. 1(c). The bucket height is now given by

$$\hat{\delta} = \begin{cases} +\left|\dfrac{\eta_0}{2\eta_1}\right| & \delta > 0 \ , \\ \\ -\left|\dfrac{\eta_0}{\eta_1}\right| & \delta < 0 \ . \end{cases} \tag{3.3}$$

Note that the height of the bucket will vanish if the lattice approaches truly isochronous ($\eta_0 = 0$).

In order that the slippage factor can be adjusted easily, the *flexible momentum-compaction module* (FMC module) proposed by Lee, Ng, and Trbojevic [1] will be used in the arcs of the collider ring. Such a module has been designed independently by Garren [2] (Fig. 2) and Ng [3] (Fig. 4) for the muon collider. Their chromaticities and transition gammas γ_t as functions of momentum offset are shown in Figs. 3 and 5, respectively.

By adjusting the negative dispersion at the ends of the FMC module, the zeroth order momentum-compaction factor α_0 can easily be tailored to receive any value between $\pm 1 \times 10^{-5}$. Within this range of α_0, the next two orders α_1 and α_2 remain almost unchanged. In order that the α-shape bucket can hold a bunch with a full momentum spread of $\delta_{\max} = \pm 0.3\%$, a minimum of $|\eta_0| = 2|\eta_1|\delta_{\max}$ is required according to Eq. (3.3). These results are listed in Table II. Therefore,

Table II: Minimum $|\eta_0|$ required to hold a bunch $\delta_{\max} = \pm 0.3\%$ in the α-shape bucket.

	η_1	η_2	$\lvert\eta_0\rvert_{\min}$
Garren	5.85×10^{-3}	2.67×10^{-2}	3.5×10^{-5}
Ng	3.20×10^{-3}	1.09×10^{-2}	1.9×10^{-5}

the limitation of $|\eta| \lesssim 1 \times 10^{-6}$ determined in Sec. II cannot be satisfied. Note that the η_1 will also contribute to the slippage factor an amount equal to $\eta_1 \delta_{\max}$ which is also larger than 1×10^{-6}. Even if we assume that the momentum spread could be compressed to $\delta_{\max} = \pm 0.01\%$ and that the bunch occupied 1/3 of the

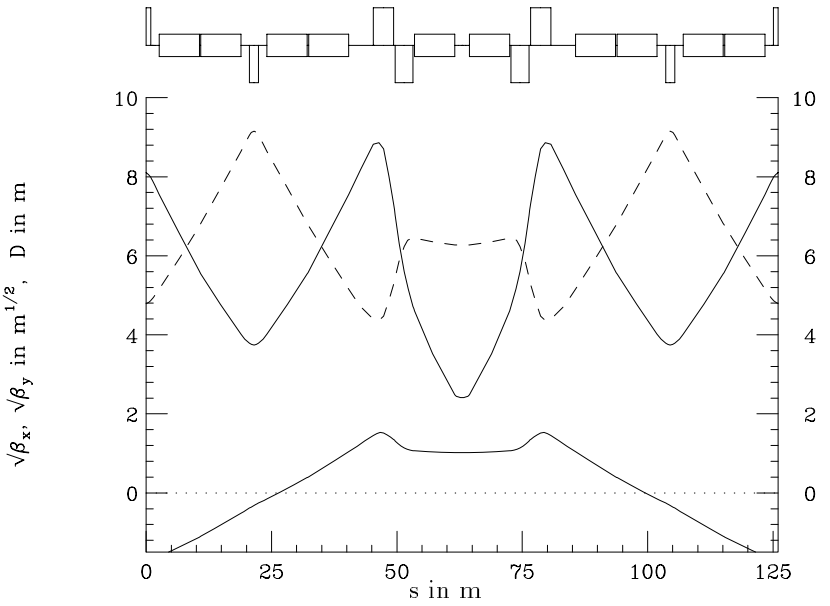

Dispersion max/min: 1.51561/−1.73050m, γ_t: (0.00, 129.807)
β_x max/min: 77.89/ 5.80332m, ν_x: 0.89598, ξ_x : − 3.44, Module length: 190.0354 m
β_y max/min: 83.83/19.28209m, ν_y: 0.53563, ξ_y : − 1.89, Total bend angle: 0.11400270 rad

Figure 2: Garren's flexible momentum-compaction module to be used in the arcs of the muon collider.

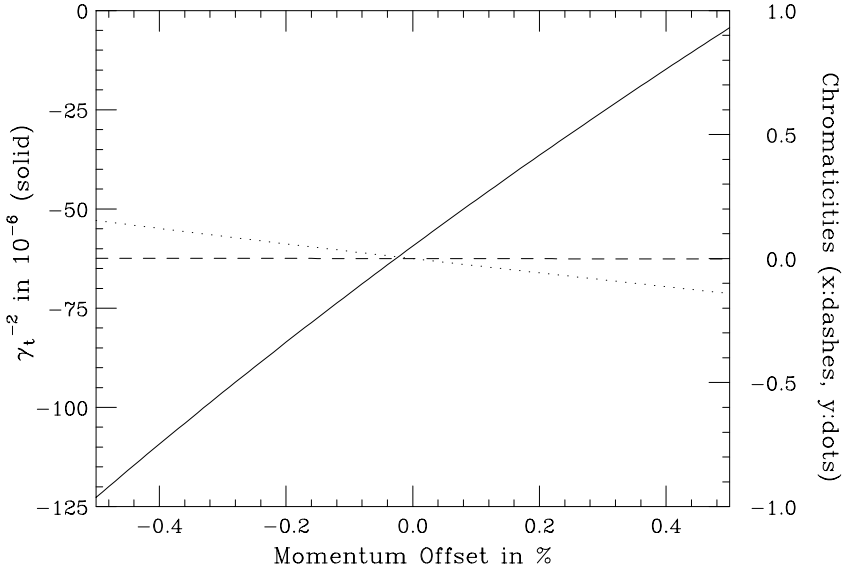

Figure 3: Variations of γ_t^{-2} and chromaticities of the Garren's module for momentum offset $\pm 0.5\%$.

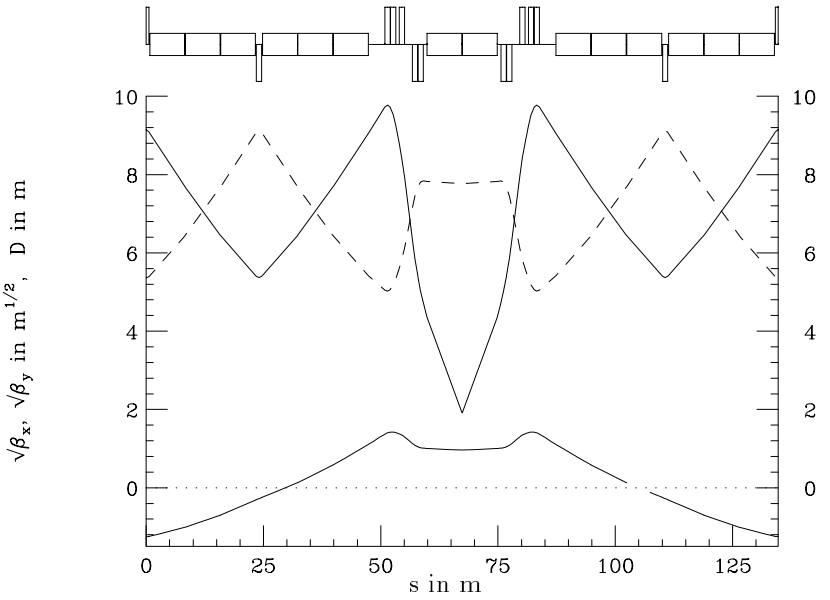

Dispersion max/min: 1.42281/−1.25140m, γ_t: (0.00, 129.8296)
β_x max/min: 95.82/ 3.67906m, ν_x: 0.75485, ξ_x : 2.91, Module length: 134.6925 m
β_y max/min: 83.43/25.27512m, ν_y: 0.47469, ξ_y : − 1.80, Total bend angle: 0.14074335 rad

Figure 4: Ng's flexible momentum-compaction module to be used in the arcs of the muon collider.

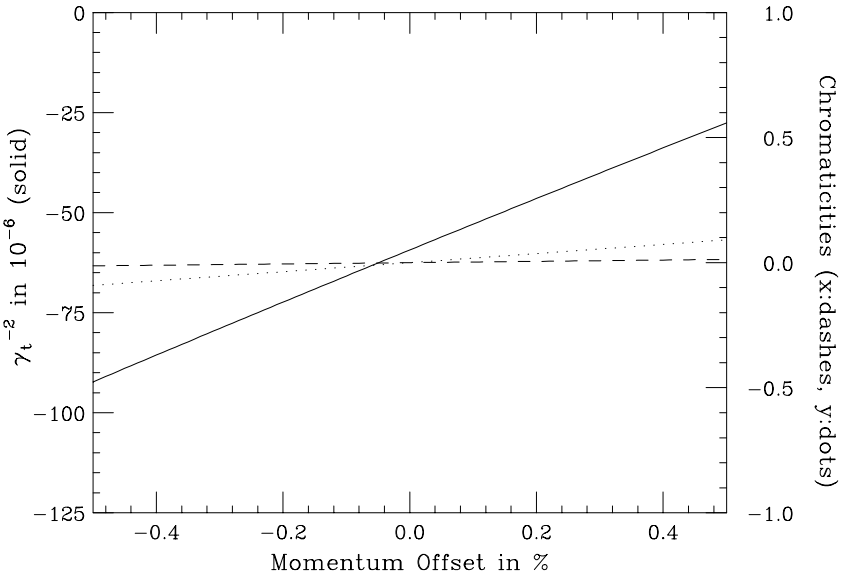

Figure 5: Variations of γ_t^{-2} and chromaticities of the Ng's module for momentum offset ±0.5%.

bucket height, we would still have $|\eta| = 3.5$ and 1.9×10^{-6}, respectively, for the Garren's and Ng's module. The small momentum aperture of the α-like bucket appears to be impractical for our muon bunches. However, there is a way to reduced η_1 so that the bucket height can be made large enough to accommodate the momentum spread of the bunch. This will be discussed in Sec. IV. Let us now review some very peculiar properties of the α-like bucket.

(1) Since the height of the α-shape bucket is fixed, the bucket width is proportional to $V^{-1/2}$ and so is the bucket area. In fact,

$$\text{Bucket half width} \quad \phi = \left(\frac{|\eta_0|^{3/2}}{|\eta_1|}\right)\left(\frac{2\pi\beta^2 hE}{3eV|\cos\phi_s|}\right)^{1/2} , \tag{3.4}$$

$$\text{Bucket area} \quad \mathcal{A} = \frac{6}{5}\left(\frac{|\eta_0|^{5/2}}{\eta_1^2}\right)\left(\frac{2\pi\beta^2 hE}{eV|\cos\phi_s|}\right)^{1/2} . \tag{3.5}$$

Therefore, contrary to the usual pendulum-like bucket, we need to lower the rf voltage in order to increase the bucket width and bucket area. As an example, if we set the bucket height to $|\eta_0/\eta_1| = k_\delta \delta_{\max}$ and the bucket half width to $\hat{\ell} = k_\ell \ell_{\max}$, the required rf voltage times rf harmonic is

$$hV = \frac{2\pi\beta^2 ER^2|\eta_0|k_\delta^2\delta_{\max}}{3ek_\ell^2\ell_{\max}^2|\cos\phi_s|} = 1698\left(\frac{k_\delta}{k_\ell}\right)^2 \text{ GV} . \tag{3.6}$$

To arrive at the numerical values, we have used $\phi_s = 0$ or π, $|\eta_0| = 1 \times 10^{-6}$, $\delta_{\max} = 0.003$, and $\ell_{\max} = 6$ mm. The maximum momentum spread and maximum length of the bunch are also related by the Hamiltonian,

$$\frac{V}{h} = \frac{\pi\beta^2 E|\eta_0|\delta_{\max}^2}{2e\sin^2\frac{1}{2}\phi_{\max}}\left(1 + \frac{2}{3k_\delta}\right) . \tag{3.7}$$

The maximum half phase spread is $\phi_{\max} = h\ell_{\max}/R = 4.71 \times 10^{-6}h$. Therefore, when the rf harmonic $h \ll 2R/\ell_{\max} = 4.23 \times 10^5$, Eqs. (3.6) and (3.7) give

$$\left(\frac{k_\delta}{k_\ell}\right)^2 = 3 + \frac{2}{k_\delta} , \tag{3.8}$$

which is universally true, independent of the bunch and lattice parameters. As a result, we have $k_\delta \gtrsim \sqrt{3}k_\ell$, and $hV \sim 5 \times 10^{12}$ V is roughly a constant. Some reasonable choices are given in Table III.

(2) There is an asymmetry between positive and negative momentum spreads due to the introduction of η_1. As a result, the bunch length will oscillate when

Table III: RF voltages, harmonics, and frequency for an α-like bucket with $\eta_0 = 1 \times 10^{-6}$ and $\hat{\delta} = |\eta_0|/\eta_1$.

$k = \hat{\delta}/\delta_{\max}$	k_ℓ	V (MV)	h	$f_{\rm rf}$ (GHz)
3	1.56	125	5×10^4	1.87
4	2.13	119	5×10^4	1.87
5	2.71	116	5×10^4	1.87
6	3.28	114	5×10^4	1.87

going from positive momentum spread to negative. Since the energy loss due to the resistive part of the impedance of the vacuum chamber is proportional to the bunch length, this may lead to a continuous growth of the synchrotron oscillation amplitude. This instability is called longitudinal head-tail, which had been observed in the CERN SPS [4]. The instability can become very strong here because η_0 has been made very small.

(3) For electron bunches, there is a strong synchrotron damping due to the emission of photons. It is possible that an electron outside the α-like bucket will be damped to attractors inside or outside the bucket without being lost. As a result, the effective bucket will be much larger than the α-like bucket given by the Hamiltonian. Figure 6 shows such a bucket enlargement for different damping coefficients [5]. However, there is no such enlargement for a muon bunch.

(4) As the amplitude of synchrotron oscillation increases, the synchrotron frequency inside the α-like bucket does not change by very much. However, it drops to zero very abruptly near the edge of the bucket. This is illustrated in Fig. 7 [5]. Thus, the α-like bucket resembles a resonance island more than the usual pendulum-like bucket. Because of the sudden drop of the synchrotron frequency near the separatrix, higher-order resonances overlap creating a thick stochastic layer. For this reason, the stable area inside the bucket will be further reduced.

IV. THE ELIMINATION OF α_1

We learn from the previous section that the η_1 term leads to a small bucket

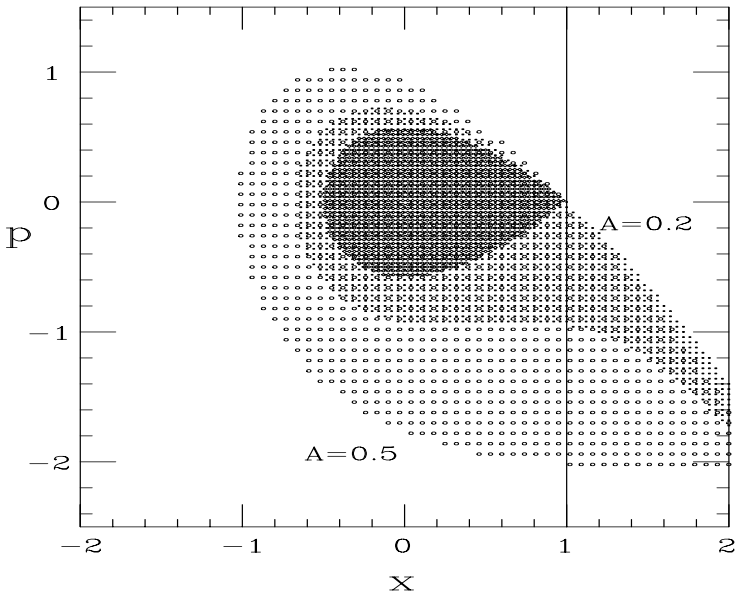

Figure 6: Particles injected into the shaded regions with damping denoted by A will eventually be damped to attractors inside or outside the α-like bucket, shown in black, 90° rotated. As a result, the effective bucket area appears to have increased.

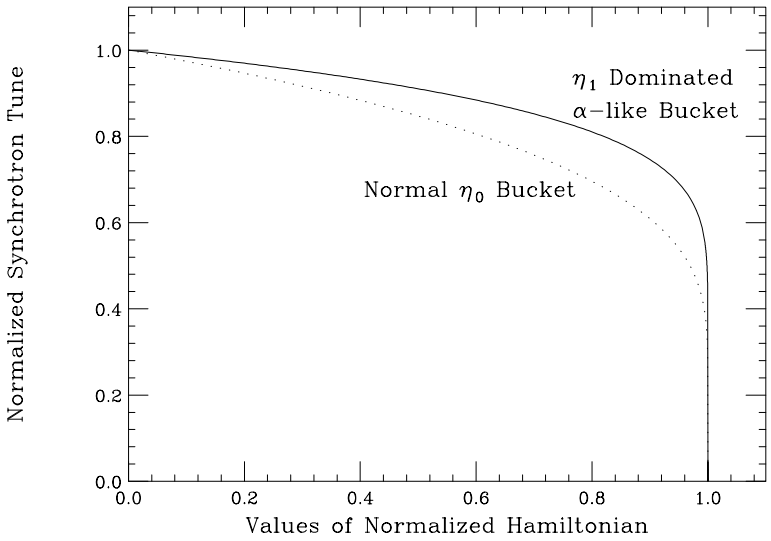

Figure 7: Normalized synchrotron tune inside the α-like bucket as a function of amplitude of oscillation. Note that the drop is very abrupt at the bucket edge corresponding to a normalized Hamiltonian of value $H = 1$. For comparison, the normalized synchrotron tune inside the usual pendulum-like bucket is shown in dots.

area and possibly longitudinal head-tail instability, thus limiting the beam dynamic when the machine is near isochronous. Furthermore, the total spread in γ_t^{-2} is rather large, $\sim 71\times10^{-6}$ for the Garren's module (Fig. 3) and $\sim 39\times10^{-6}$ for the Ng's module (Fig. 5) for a momentum spread of $|\delta| < 0.3\%$. A large spread in γ_t^{-2} implies large slippage factors for some beam particles, so that unusually large rf will be required for bunching. Therefore, it may be a good idea to eliminate the η_1 term. The Hamiltonian then becomes

$$H = \left(\frac{\eta_0\delta^2}{2} + \frac{\eta_2\delta^4}{4}\right) h\omega_0 + \frac{eV\omega_0}{2\pi\beta^2 E}\left[\cos(\phi_s+\Delta\phi) + \Delta\phi\sin\phi_s\right] , \qquad (4.1)$$

where the next nonlinear term, η_2, has been included.

A quadrupole bends particles with positive and negative off-momenta in opposite directions. To lowest order, it contributes to α_0 of the momentum-compaction factor defined in Eq. (2.7). On the other hand, a sextupole bends particles with positive and negative off-momenta in the same direction. Therefore, to lowest order, it contributes to α_1. In other words, sextupoles can be used to modify α_1 or η_1. A simplified lattice consisting of only FODO cells of thin quadrupoles and dipoles filling all spaces is exactly soluble. With thin sextupoles of integrated strengths

$$S_F = \int d\ell \frac{B''_{S_F}}{2(B\rho)} \qquad S_D = \int d\ell \frac{B''_{S_D}}{2(B\rho)} \qquad (4.2)$$

inserted, respectively, at the F and D quadrupoles, the effect on α_1 is [6]

$$\Delta\alpha_1 = -S_F\hat{D}_0^3 - S_D\check{D}_0^3 , \qquad (4.3)$$

where $\hat{D}_0$ and $\check{D}_0$ are, respectively, the zero-order dispersions at the focusing and defocusing quadrupoles, and every quantity in the equation that carries a dimension is normalized to the half length of the FODO cell. To cancel the natural chromaticities, S_F is chosen positive for the FODO lattice while S_D negative. Thus S_F reduces α_1 while S_D increases it.

We hope that Eq. (4.3) would also apply to the FMC module. To cancel α_1, we therefore employ only S_F. The chromaticities left behind or created will only be a tiny fraction of the huge natural chromaticities of the low-beta at the interaction region, and can therefore be taken care of easily by the chromatic sextupoles there.

We place a pair of S_F sextupoles just outside the low-beta quadrupoles of the FMC module, where the horizontal betatron function and the dispersion are near maximum. By adjusting the strength of the sextupoles, the variation of the slippage factor η as a function of momentum offset changes from nearly linear in Fig. 3 to parabolic in Fig. 8 for Garren's module. Since the antisymmetric part of η is no longer present in Fig. 8, we conclude that the contribution of η_1 has been eliminated. Note that the total spread of η is only 2.0×10^{-6} for a momentum spread of $\pm 0.5\%$, and 0.6×10^{-6} for a momentum spread of $\pm 0.3\%$.

Similar process can be performed onto the Ng's module, resulting in a parabolic variation of the momentum-compaction factor as shown in Fig. 9. Here, the total spread of η is only 0.8×10^{-6} for a momentum spread of $\pm 0.5\%$, and 0.3×10^{-6} for a momentum spread of $\pm 0.3\%$. The spread in η appears to be less than that for the Garren's module. This may be due to the fact that weaker quadrupoles have been used in the Ng's module.

Strictly speaking, what are plotted in Figs. 3, 5, 8, and 9 are not slippage factors but γ_t^{-2} instead. The latter is defined as

$$\gamma_t^{-2} = \frac{p}{C}\frac{dC}{dp} \ , \tag{4.4}$$

In a power series expansion,

$$\gamma_t^{-2} = a_0 + a_1\delta + a_2\delta^2 + \cdots \ , \tag{4.5}$$

the expansion coefficients are related to the various orders of the momentum-compaction factor by

$$\begin{aligned} a_0 &= \alpha_0 \ , \\ a_1 &= 2\alpha_1 + \alpha_0 - \alpha_0^2 \ , \\ a_2 &= 3\alpha_2 + 2\alpha_1 - 3\alpha_0\alpha_1 - \alpha_0^2 + \alpha_0^3 \ . \end{aligned} \tag{4.6}$$

For $|\alpha_0 + \alpha_1\delta + \alpha_2\delta^2| \lesssim 10^{-6}$, we have for the requirements of the α-like bucket,

$$\left\{ \begin{array}{l} |\alpha_1\delta| \sim |\alpha_0| \ , \\ |\alpha_2\delta| \ll |\alpha_1| \ , \end{array} \right. \Longrightarrow \left\{ \begin{array}{l} |a_1\delta| \sim 2|a_0| \ , \\ |a_2\delta| \ll \frac{3}{2}|a_1| \ , \end{array} \right. \tag{4.7}$$

The elimination of the η_1 term is equivalent to having

$$\left\{ \begin{array}{l} |\alpha_1\delta| \ll |\alpha_0| \ , \\ |\alpha_1| \ll |\alpha_2\delta| \ , \end{array} \right. \Longrightarrow \left\{ \begin{array}{l} |a_1\delta| \ll 2|a_0| \ , \\ |a_1| \ll \frac{2}{3}|a_2\delta| \ , \end{array} \right. \tag{4.8}$$

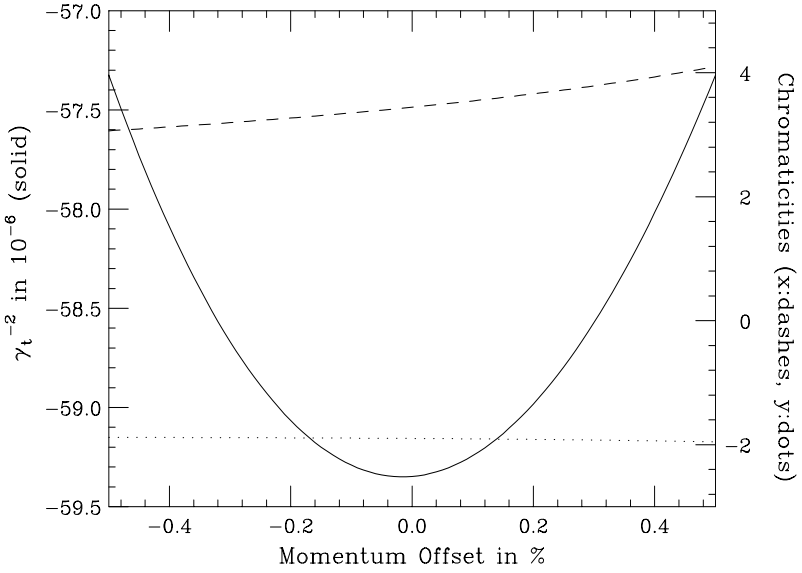

Figure 8: Variations of γ_t^{-2} and chromaticities of the Garren's module for momentum offset $\pm 0.5\%$.

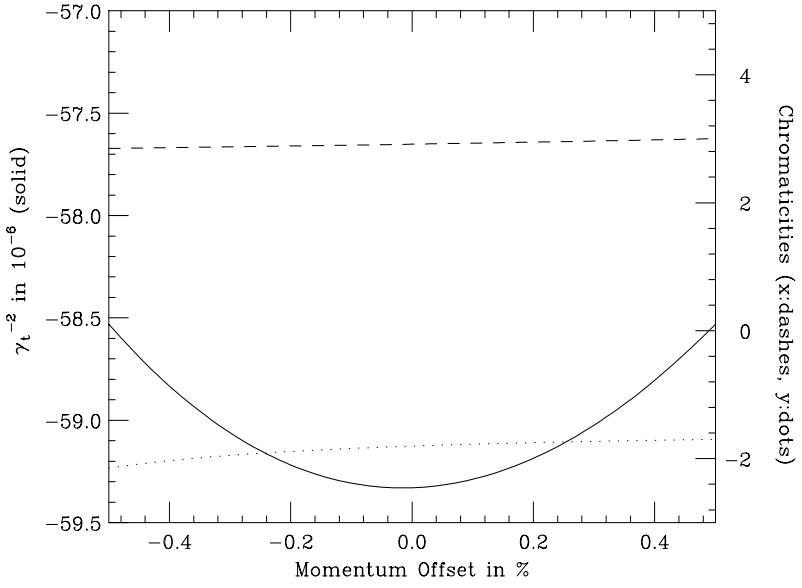

Figure 9: Variations of γ_t^{-2} and chromaticities of the Ng's module for momentum offset $\pm 0.5\%$.

which is just the elimination of the linear term in γ_t^{-2}.

V. THE η_2-DOMINATED BUCKET

With the contribution of η_1 eliminated, It is possible to adjust η_0 to zero so that the Hamiltonian becomes

$$H = \frac{1}{4}h\omega_0\eta_2\delta^4 + \frac{eV\omega_0}{2\pi\beta^2 E}\left[\cos(\phi_s + \Delta\phi) + \Delta\phi\sin\phi_s\right] , \tag{5.1}$$

Now for $\phi_s = 0$, the bucket looks pendulum-like with the usual width of $\Delta\phi = 2\pi$. The bucket half height is

$$\hat{\delta} = \left(\frac{4eV}{\pi\beta^2 E h|\eta_2|}\right)^{1/4} . \tag{5.2}$$

When the half bunch length $\ell_{\max}$ is short, it is related to the half momentum spread $\delta_{\max}$ by

$$\delta_{\max}^4 = \left(\frac{eVh}{\pi\beta^2 E|\eta_2|}\right)\left(\frac{\ell_{\max}}{R}\right)^2 , \tag{5.3}$$

where $2\pi R$ is the ring circumference. If we let k denote the ratio of the bucket height to the momentum spread of the bunch, or $\hat{\delta} = k\delta_{\max}$, we can solve for the necessary rf voltage and rf harmonic:

$$V = \frac{\pi\beta^2 E R k^2 \Delta\eta\delta^2}{2\ell_{\max}} , \tag{5.4}$$

$$h = \frac{2R}{\ell_{\max}k^2} , \tag{5.5}$$

where $\Delta\eta = |\eta_2|\delta_{\max}^2$ is desired spread of slippage factor of the bunch. If we let $\Delta\eta = 1\times10^{-6}$, $\delta_{\max} = 0.003$, and $\ell_{\max} = 6$ mm, the required rf voltages for various values of k are obtained and are listed in Table IV.

The rf voltages appear high but attainable. Note that the rf voltage is proportional to $\Delta\eta$, the desired spread in momentum-compaction, and $\delta_{\max}^2$, the momentum spread of the bunch squared. Thus, the rf voltage can be reduced by a factor of 10, if we reduce the momentum-compaction spread to $\Delta\eta = 1\times10^{-7}$. On the other hand, the rf frequency is independent of the choice of $\Delta\eta$ and $\delta_{\max}$.

For small phase spread, Eq. (5.1) describes a particle oscillating in a quartic potential (with $\Delta\phi$ and δ interchanged). This is a well-known situation when a

Table IV: RF voltages, harmonics, and frequency for an η_2-dominated lattice with $\Delta\eta = 1 \times 10^{-6}$.

$k = \hat{\delta}/\delta_{\max}$	V (MV)	h	$f_{\rm rf}$ (GHz)
3	54.0	4.72×10^4	1.77
4	96.0	2.65×10^4	0.99
5	150.0	1.70×10^4	0.64
6	216.0	1.18×10^4	0.44

second higher harmonic cavity is present and the two cavity voltages are inversely proportional to the square of their respective harmonics. For such a system, the synchrotron frequency is zero at zero oscillating amplitude and increases linearly with respect to the momentum offset δ, or the 4th root of the Hamiltonian. The synchrotron frequency increases to a maximum for larger oscillation amplitude and drops to zero again at the edge of the bucket. Simple derivation gives the synchrotron tune

$$\nu_s = \nu_{s0} F(H) \ , \tag{5.6}$$

where

$$\nu_{s0} = \sqrt{\frac{h\Delta\eta eV}{2\pi\beta^2 E}} \qquad \Delta\eta = |\eta_2|\delta^2 \tag{5.7}$$

is just the synchrotron tune at a spread of slippage factor $\Delta\eta$, and the form factor $F(H)$ can be written as

$$F^{-1}(H) = \frac{2^{3/4}}{2\pi} \int_0^{\pi/2} \frac{dz}{\sqrt{\cos z}\sqrt{1 - \sin^2\frac{\phi}{2}\sin^2 z}} \ . \tag{5.8}$$

The form factor is evaluated at the Hamiltonian value,

$$H = \frac{eV\omega_0}{\pi\beta^2 E}\sin^2\tfrac{\phi}{2} = \tfrac{1}{4}h|\eta_2|\omega_0\delta^4 \ , \tag{5.9}$$

where ϕ and δ equal to, respectively, the phase and momentum-offset excursions of the beam particle under investigation. This is plotted in Fig. 10. A large spread in synchrotron frequency can be advantageous to providing Landau damping to mode-coupling instabilities. For a designed slippage spread of $\Delta\eta = 1 \times 10^{-6}$ and a bunch of maximum half length $\ell_{\max} = 6$ mm and momentum spread

$\delta_{\max} = 0.003$, we obtain with the aid of Table III, the maximum synchrotron tune $\nu_s = 0.64 \times 10^{-3}$, which occurs at the edge of the bunch and is almost independent of what k is used. Thus, for 1000 turns in the muon collider, a particle makes at the most 0.64 synchrotron oscillation if $\Delta\eta = 1 \times 10^{-6}$.

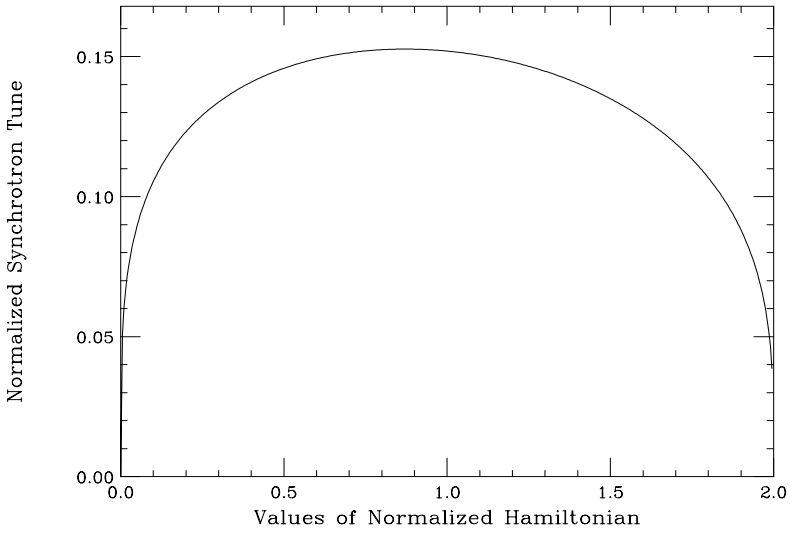

Figure 10: Synchrotron oscillation frequency inside a η_2-dominated bucket. The abscissa is in value of the Hamiltonian which is normalized to 2 at the edge of the bucket.

VI. THE η_0-DOMINATED QUASI-ISOCHRONOUS BUCKET

It is also possible to eliminate the contributions of η_1 and η_2, so that there will not be any slippage spread for the off-momentum particles. A closer look of Fig. 3 and 5 reveals that the γ_t^{-2} curves are bulging upward or the coefficients a_2 of the parabolic terms in Eq. (4.5) are negative. However, after the sextupole corrections, we find $a_2 > 0$ in both Fig. 8 and 9. This implies that the sextupoles not only reduce a_1, but increase a_2 at the same time. In fact, if the study of sextupoles on momentum-compaction factor in Ref. 5 is extended to another order of δ, we will find that, similar to Eq. (4.3), the correction to α_2 includes terms proportional to S_F^2 and S_D^2, and these terms are positive. In other words,

the sextupoles talk to each other. Therefore the correction to a_2 will be sensitive to the locations of the sextupoles.

In addition to the sextupole pair placed at the low-beta quadrupoles, another pair of sextupoles can be placed next to the F quadrupoles at the module ends (see Fig. 2). By choosing appropriate strengths for the different sextupole families, one can flatten the parabolic behavior of γ_t^{-2} in Fig. 8, so that the contributions of both a_1 and a_2 vanish [7]. From the discussion near the end of Sec. IV, this is equivalent of eliminating the contributions of both α_1 and α_2

Another way to control a_2 without generating a contribution to the a_1 is to pair sextupoles separated by phase intervals of π in the arcs. For example, moving the two sextupoles from the Garren's module from just outside the low-beta quadrupoles to inside the low-beta quadrupoles, one can reduce the contribution of a_2 by almost one order of magnitude [8].

With the elimination of the contributions of η_1 and η_2, the Hamiltonian becomes the familiar

$$H = \frac{h\omega_0\eta_0\delta^2}{2} + \frac{eV\omega_0}{2\pi\beta^2 E}\left[\cos(\phi_s + \Delta\phi) + \Delta\phi\sin\phi_s\right] . \tag{6.1}$$

For synchrotron phase $\phi_s = 0$, we have the usual pendulum-like bucket whose height $\hat{\delta}$ can be derived easily,

$$\hat{\delta}^2 = \frac{2eV}{\pi\beta^2 E h|\eta_0|} . \tag{6.2}$$

For a small bunch, the half length $\ell_{\max}$ and the half momentum offset $\delta_{\max}$ are related by

$$\delta_{\max}^2 = \frac{eVh}{2\pi\beta^2 E|\eta_0|}\left(\frac{\ell_{\max}}{R}\right)^2 . \tag{6.3}$$

If we let $\hat{\delta} = k\delta_{\max}$, the rf voltage and rf harmonic can be solved:

$$V = \frac{\pi\beta^2 E|\eta_0|\delta^2 k}{e\ell_{\max}} , \tag{6.4}$$

$$h = \frac{2R}{k\ell_{\max}} . \tag{6.5}$$

With $|\eta_0| = 1\times10^{-6}$, $\delta_{\max} = 0.003$, and $\ell_{\max} = 6$ mm, the results are tabulated in Table V for various values of k.

We see that the rf voltages are of the same order of magnitude as in Table IV for the η_2-dominated bucket, and are in fact a bit less. The synchrotron tune is

Table V: RF voltages, harmonics, and frequency for an η_0-dominated lattice with $\eta = 1 \times 10^{-6}$.

$k = \hat{\delta}/\delta_{\max}$	V (MV)	h	$f_{\rm rf}$ (GHz)
3	36.0	4.72×10^4	1.77
4	48.0	2.65×10^4	0.99
5	60.0	1.70×10^4	0.64
6	72.0	1.18×10^4	0.44

independent of k and is given by

$$\nu_s = \sqrt{\frac{h|\eta_0|V}{2\pi\beta^2 E}} = \frac{|\eta_0|\delta_{\max}R}{\ell_{\max}} = 0.637 \times 10^{-3} \ , \tag{6.6}$$

which is also comparable to that for the η_2-dominated bucket. For this reason, there is no need to eliminate the η_2 term. We only need to control it so that the total slippage factor is within the design value; for example,

$$|\eta_0 + \eta_2\delta_{\max}^2| \lesssim 1 \times 10^{-6} \ . \tag{6.7}$$

VII. RELIABILITY OF α_1 AND α_2

Sections IV and V deal with the corrections to the higher-order terms of γ_t^{-2} by inserting sextupoles. Naturally, we need to ask how accurate α_1 and α_2 are as computed by lattice codes. In SYNCH [9], the off-momentum closed orbit is obtained by first tracking an initial "first guess" particle state vector V_0 through one complete revolution so as to produce a new state vector V_1. These state vectors are 7-element vectors; for example,

$$V = (x, x', y, y', -ds, dp/p, 1) \ , \tag{7.1}$$

where the first 4 entries are for the horizontal and vertical deviations and slopes, the 5th denotes the shortening in orbit length, the 6th momentum offset, and the 7th is reserved for misalignment calculation. The transfer matrices of the ring's elements are then linearized about this initial single-turn trajectory, generating new transfer matrices, R, and a linearized single-turn transfer matrix $T = R_N R_{N-1} \cdots R_2 R_1$.

On may now track a particle vector X_0 in a small neighborhood of V_0 so that $X_0 = V_0 + Z_0$. After one revolution, this vector becomes $X_1 = V_1 + Z_1$, where $Z_1 = TZ_0$. If X_0 is a closed orbit, we must have $X_0 = X_1$, or

$$X_0 = V_0 + Z_0 = V_1 + Z_1 \ . \tag{7.2}$$

Therefore,

$$X_0 = V_1 + TZ_0 = V_1 + T(X_0 - V_0) \ , \tag{7.3}$$

or the closed orbit is

$$X_0 = -(T + I)^{-1}(V_1 - V_0) \ , \tag{7.4}$$

where I is the identity matrix.

The length of the closed orbit found in this way should include the wiggling term which takes care of the fact that the off-momentum closed orbit is not parallel to the on-momentum closed orbit. The linearization around the closed orbit will allow the lowest order calculation of the transition gamma at that particular momentum offset. In other words, γ_t^{-2} will be accurate up to the a_1 term. Therefore, we expect α_1 should be computed accurately by SYNCH. In fact, a numerical comparison had been made in Ref. 5 with the theoretical results of a simplified FODO lattice with only thin quadrupoles and with dipoles filling all spaces. For example, the computed effect of sextupoles on α_1 is shown in Eq. (4.3). The agreements have been excellent, up to at least 3 figures for various quadrupole strengths and number of FODO cells. This does not, however, exclude the possibility of a disagreement with thick quadrupoles, because the exact integration of the particle trajectory inside a quadrupole is tedious and time consuming, and lattice codes usually resort to approximations. Nevertheless, quadrupoles are usually short compared with dipoles and the bend field is usually weak when the radial offset is small. Therefore, it is reasonable to hope that the approximations would not introduce much error.

Because of the linearization of the transfer matrix at the off-momentum closed orbit, we do not expect the next higher order in δ will be taken into account correctly. As a result, a_2 and α_2 will not be computed correctly by SYNCH. Here, we look into the simplified FODO lattice made up of 300 identical FODO cells each with a phase advance of $\mu = 2\sin^{-1}\frac{1}{2}$. By offsetting the momentum by ± 0.0001 in small steps, the values of the γ_t^{-2} computed by SYNCH are fitted

to a polynomial of degree two, with the three coefficients: $a_0 = 0.00171503$, $a_1 = 0.00705748$, and $a_2 = 0.00848989$. The corresponding coefficients of the momentum-compaction factor are listed in Table VI along with the analytically computed values. Analytic formulas for α_2 together with its effect from sextupoles have been derived in this simple model. However, they are rather lengthy and complicated, and are therefore omitted here. It is obvious that α_2 has not been given correctly by SYNCH. We also tried to fit γ_t^{-2} obtained from SYNCH to a polynomial of degree 3; the first three α's do not change in their first 4 significant figures.

Table VI: Comparison of SYNCH and theoretical results for the simplified FODO lattice.

	SYNCH	Theory
α_0	0.00171503	0.00171518
α_1	0.00267272	0.00267273
α_2	0.00105371	-0.00009099

With α_2 not predictable with lattice codes and difficult to calculate theoretically for the FMC module, we must resort to measurements [10]. The slippage factor can be inferred by the synchrotron tune of a particle in an off-momentum orbit. This can be done by altering the rf frequency from $f_{\rm rf}$ by an amount $\Delta f_{\rm rf}$ so that the synchronous particle is in a different closed orbit of length $C_0 + \Delta C$ at a momentum $p_0 + \Delta p = p_0\delta_0$. The phase equation per turn of Eq. (2.8) becomes

$$\frac{d\Delta\phi}{dn} = 2\pi\eta(\delta)(\delta - \delta_0) \ . \tag{7.5}$$

This is because the synchronous particle which is at $\delta = \delta_0$ should have zero phase slip. With $\Delta\delta = \delta - \delta_0$, Eq. (7.5) can be rewritten as

$$\frac{d\Delta\phi}{dn} = 2\pi \left[\eta(\delta_0)\Delta\delta + \eta'(\delta_0)\Delta\delta^2 + \tfrac{1}{2}\eta''(\delta_0)\Delta\delta^3 + \cdots \right] \ . \tag{7.6}$$

Thus the synchrotron tune becomes

$$\nu_s = \nu_{s0}\left(\frac{\eta(\delta_0)}{\eta_0}\right)^{1/2} = \nu_{s0}\left[1 + \frac{\eta_1}{2\eta_0}\delta_0 + \left(\frac{\eta_2}{2\eta_0} - \frac{\eta_1^2}{8\eta_0^2}\right)\delta_0^2 + \cdots \right] \ , \tag{7.7}$$

where ν_{s0} is the synchrotron tune for the on-momentum particle when $\eta = \eta_0$. From Eq. (2.7), the momentum offset can be written in terms of the orbit-length offset,

$$\delta_0 = \frac{\Delta C}{\alpha_0 C_0} - \frac{\alpha_1}{\alpha_0}\left(\frac{\Delta C}{\alpha_0 C_0}\right)^2 + \cdots \ . \tag{7.8}$$

Since $\Delta C/C_0 = -\Delta f_{\rm rf}/f_{\rm rf}$, substituting Eq. (7.8) into Eq. (7.7), we arrive at

$$\nu_s = \nu_{s0}\left[1 - \frac{\eta_1}{\eta_0^2}\left(\frac{\Delta f_{\rm rf}}{f_{\rm rf}}\right) - \left(\frac{5\eta_1^2}{8\eta_0^4} - \frac{\eta_2}{2\eta_0^3}\right)\left(\frac{\Delta f_{\rm rf}}{f_{\rm rf}}\right)^2 + \cdots\right] \ , \tag{7.9}$$

where we have used $\eta_0 \approx \alpha_0$ and $\eta_1 \approx \alpha_1$.

The maximum momentum spread of the designed muon bunch is $\delta_{\rm max} = 0.003$ and $\eta \approx 1\times10^{-6}$. Therefore a variation of the rf frequency by $\Delta f_{\rm rf}/f_{\rm rf} \approx 3\times10^{-9}$ will be required. Since the figure of merit of a superconducting cavity can easily reach $Q = 1 \times 10^9$, such an rf frequency variation should be possible.

A low-intensity proton bunch with small momentum spread is injected into the muon collider for the measurement. The on-momentum synchrotron tune will give η_0. The higher orders η_1 and η_1 can be inferred by measuring the synchrotron tune as a function of $\Delta f_{\rm rf}/f_{\rm rf}$. If no asymmetric variation of the synchrotron tune is observed when $\Delta f_{\rm rf}/f_{\rm rf}$ varies between $\pm 3 \times 10^{-9}$, we can conclude that the η_1 contribution is insignificant in this collider lattice. Furthermore, if the synchrotron tune remains flat during the variation of $\Delta f_{\rm rf}/f_{\rm rf}$, the η_2 contribution is also insignificant. The bucket will then be η_0-dominated. However, if we see a parabolic dependency of ν_s versus $\Delta f_{\rm rf}/f_{\rm rf}$, we can tune the machine so that η_0 becomes zero. The bucket will then be η_2-dominated and the magnitude of η_2 can be determined easily.

Strictly speaking, Eqs. (7.7) to (7.9) are not valid when the contribution η_0 is small. Under that situation, we can write

$$\nu_s = \left(\frac{heV}{2\pi\beta^2 E}\right)^{1/2}[\eta_0 + \eta_1\delta_0 + \eta_2\delta_0^2]^{1/2} \ , \tag{7.10}$$

and solve for δ_0 in terms of $\Delta C/C_0$ exactly from Eq. (2.7). After substituting the result into Eq. (7.10), we will then obtain ν_s in terms of $\Delta f_{\rm rf}/f_{\rm rf}$ which is valid for all values of η_0, η_1, and η_2. For example, when the contribution of η_2 overshadows those of η_0 and η_1, we have,

$$\nu_s = \left(\frac{heV}{2\pi\beta^2 E}\right)^{1/2}\eta_2^{1/3}\left|\frac{\Delta f_{\rm rf}}{f_{\rm rf}}\right|^{2/3} \ , \tag{7.11}$$

except when $\Delta f_{\rm rf}/f_{\rm rf}$ is very close to zero. Similarly, for an α-like bucket [11],

$$\nu_s = \left(\frac{heV}{2\pi\beta^2 E}\right)^{1/2} \left[\frac{\eta_0}{2} + \sqrt{\frac{\eta_0^2}{4} - \eta_1 \frac{\Delta f_{\rm rf}}{f_{\rm rf}}}\right] \ . \tag{7.12}$$

VIII. MICROWAVE INSTABILITY

Since the muon collider is supposed to operate near transition with the slippage factor $|\eta| \approx 1 \times 10^{-6}$, the muon bunches will be susceptible to microwave instability due to the lack of sufficient Landau damping. When the Hamiltonian is η_0-dominated, the allowable longitudinal coupling impedance of the vacuum chamber for stability is given by the Boussard-modified Keil-Schnell criterion [12]:

$$\left|\frac{Z_{||}}{n}\right| \lesssim \left(\frac{2\pi|\eta_0|\beta^2 E}{eI_p}\right)\sigma_\delta^2 \ , \tag{8.1}$$

where a bi-Gaussian distribution of the bunch shape has been assumed and

$$I_p = \frac{eN}{\sqrt{2\pi}\sigma_\tau} \tag{8.2}$$

is the local peak current of 12.78 kA for a bunch consisting of $N = 2\times10^{12}$ muons and an rms bunch length of $\sigma_\tau = 10$ ps and rms momentum spread $\sigma_\delta = 0.0015$. This amounts to a limit of $|Z_{||}|/n \lesssim 0.0022$ Ohms, which is way too small to be implemented. Equation (8.1) can be rewritten as

$$n\omega_0\sqrt{\frac{eI_p|Z_{||}/n||\eta_0|}{2\pi\beta^2 E}} \lesssim n\omega_0|\eta_0|\sigma_\delta \ . \tag{8.3}$$

The left side is the growth rate of microwave instability and the right side is rate of Landau damping coming from the spread in frequency. For microwave instability to occur, the wavelength of the disturbance must be less than the size of the bunch. One estimation is a wavelength less than about 4 to 6 times the rms bunch length of $\sigma_\ell = 3$ mm, which is equivalent to a frequency larger than 16 to 25 GHz. Another estimation is to take a frequency which is larger than the rms bunch spectrum frequency, which is $\sigma_f = 1/(2\pi\sigma_\tau) = 15.6$ GHz. Therefore, roughly the Landau damping time is $1/(2\pi n|\eta_0|\sigma_\delta) \approx 250$ turns. Since this is shorter than the storage time of ~ 1000 turns in the collider ring, the stability criterion of Eq. (8.1) or (8.3) must be satisfied.

One may argue that the usual broad-band model has the impedance centered around cutoff frequency. Therefore $Z_{||}/n$ must drop down tremendously at the high frequencies that are responsible for microwave instability. However, the designed pipe radius of the collider is $b = 1.5$ cm. With c denoting the velocity of light, the cutoff frequency is therefore already $f_c = 2.405\, c/(2\pi b) = 7.65$ GHz, which is not much lower than the ~ 15 GHz that we talked about. Remember that the broad-band model is only a model and the impedance may not actually be centered right at cutoff.

Let us investigate the possibility of having a reasonable amount of impedance above 15 GHz. Henke [13] had computed analytically the impedance of a small pill-box cavity. With a depth to pipe radius ratio of $\Delta/b = 0.1$ and width to pipe radius $2g/b = 0.01$, the real part of the longitudinal impedance is shown [14] in Fig. 11. We see a roughly a broad band with a peak value of $\sim 10\ \Omega$. It is centered at $\omega b/c \approx 15$ or 48 GHz, which corresponds to about a half wavelength into the cavity depth. For a collider ring circumference of 8000 m, this amounts to $\mathcal{R}e\, Z_{||}/n \approx 7.9 \times 10^{-6}\ \Omega$. Note that this cavity depth is, in fact, $\Delta = 1.5$ mm and width $2g = 0.15$ mm; so it is like a scratch in the beam pipe. If we add up a lot of such "scratches" or small dings and bugglings for the whole vacuum chamber, the total $\mathcal{R}e\, Z_{||}/n$ can be appreciable.

In Fig. 12, we plot the real part of the impedance for the same pill-box cavity with depth increased to $\Delta/b = 0.2$ and the total width increased to $2g/b = 0.2$. We see two broad peaks. The first one peaks at roughly 25 Ω around $\omega b/c \approx 6$ or ~ 19 GHz, corresponding to $\mathcal{R}e\, Z_{||}/n \approx 5 \times 10^{-5}\ \Omega$. This is a cavity of depth $\Delta = 3$ mm and width $2g = 3$mm. The small pill-box like cavity left behind by a shield bellows system can be of such a size. Assuming 1000 bellows systems for the more than a thousand elements, the impedance is therefore $\mathcal{R}e\, Z_{||}/n \approx 0.05\ \Omega$. In an earlier design of the sliding shielded bellows of the Superconducting Super Collider, the pill-box like cavity left behind has a depth of $\Delta = 4$ mm and a width of as much as $2g = 10$ cm when the vacuum chamber is at superconducting temperature. Such a system gives a broad-band impedance [15] of $\sim 40\ \Omega$ at 15 GHz. For 1000 such bellows in the muon collider, the impedance adds up to $\mathcal{R}e\, Z_{||}/n \approx 0.1\ \Omega$.

There must also be some other small discontinuities in the vacuum chamber.

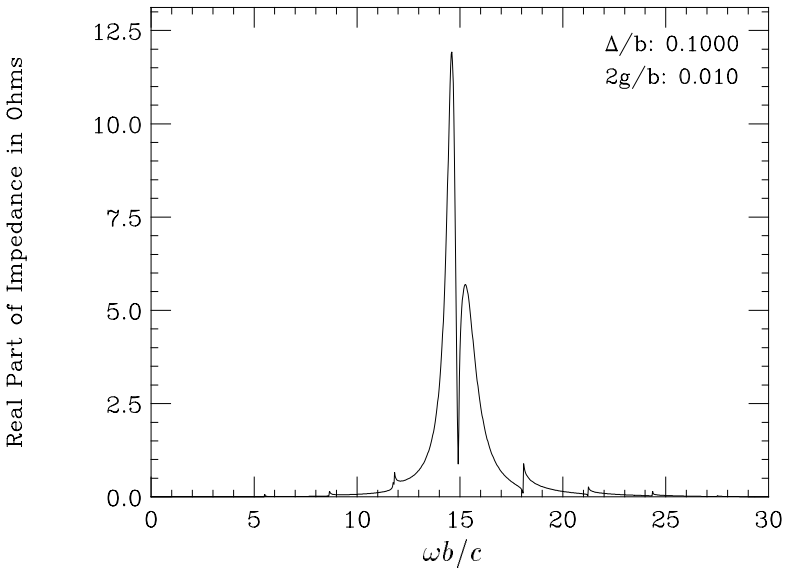

Figure 11: Real part of longitudinal impedance as a function of $\omega b/c$ for a pill-box cavity of depth $\Delta = 0.1\,b$ and length $2g = 0.01\,b$, where b is the radius of beam pipe and $\omega/2\pi$ is the frequency.

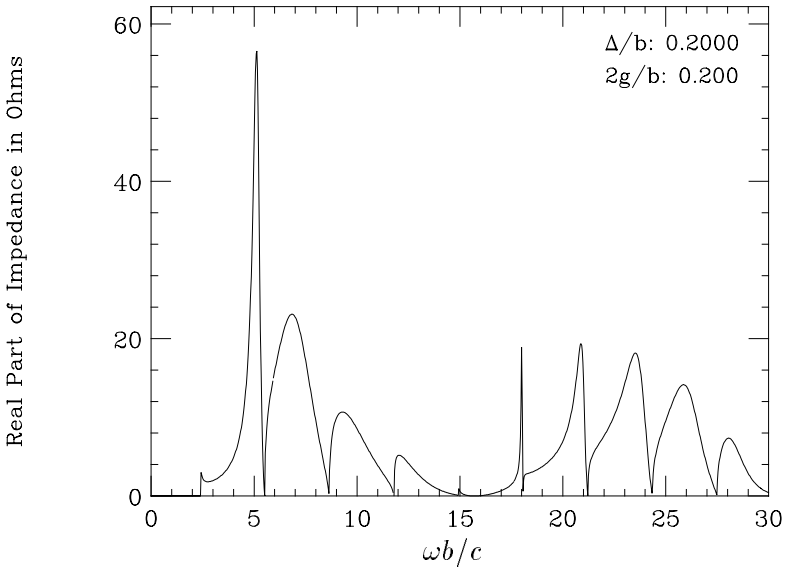

Figure 12: Real part of longitudinal impedance as a function of $\omega b/c$ for a pill-box cavity of depth $\Delta = 0.20\,b$ and length $2g = 0.20\,b$, where b is the radius of beam pipe and $\omega/2\pi$ is the frequency.

As a result, it is not unreasonable to assume that a $Z_{||}/n$ of magnitude from 0.1 to 1.0 Ω will be driving the microwave instability in the muon collider ring. According to Eq. (8.3), the growth time at 15 GHz is therefore 12.5 to 39.5 turns.

For a η_2-dominated bucket, we need an extension of Keil-Schnell criterion. Notice that Eq. (8.1) can be rewritten as

$$\left(\frac{2eI_p|Z_{||}/n|}{\pi\beta^2|\eta_0|E}\right)^{1/2} \lesssim 2\sigma_\delta \ . \tag{8.4}$$

The left side is the height of a bucket driven by a voltage $I_p|Z_{||}|$ at harmonic n. Stability implies that this bucket height must be less than $2\sigma_\delta$ or roughly the half momentum spread $\delta_{\max}$. This is called self-bunching. Now we can generalize this idea of self-bunching to the η_2-dominated bucket. Using the bucket height given by Eq. (5.2), we obtain the condition of avoiding self-bunching as

$$\left(\frac{4eI_p|Z_{||}/n|}{\pi\beta^2|\eta_2|E}\right)^{1/4} \lesssim 2\sigma_\delta \ . \tag{8.5}$$

Therefore, the impedance limit for microwave instability becomes

$$\left|\frac{Z_{||}}{n}\right| \lesssim \left(\frac{\pi|\eta_2|\beta^2E}{eI_p}\right)4\sigma_\delta^4 \ . \tag{8.6}$$

This can be obtained from Eq. (8.1) by the replacement

$$|\eta_0| \longrightarrow 2|\eta_2|\sigma_\delta^2 \approx \frac{1}{2}\Delta\eta \ , \tag{8.7}$$

where we have assumed $\delta_{\max} \approx 2\sigma_\delta$ and the spread of slippage factor $\Delta\eta = |\eta_2|\delta_{\max}^2$. Thus, the impedance limitation here is only $\frac{1}{2}$ that for the η_0-dominated bucket.

Next, let us examine the α-like bucket. When the driving impedance is small, the particles will self-bunch into pendulum-like buckets as shown in Fig. 13a. Again, when the height of the pendulum-like buckets is larger than the momentum spread of the bunch, we have microwave growth. Therefore, for no growth we require, according to Eq. (8.4),

$$\left(\frac{2eI_p|Z_{||}/n|}{\pi\beta^2|\eta_0|E}\right)^{1/2} \lesssim \sigma_\delta \ . \tag{8.8}$$

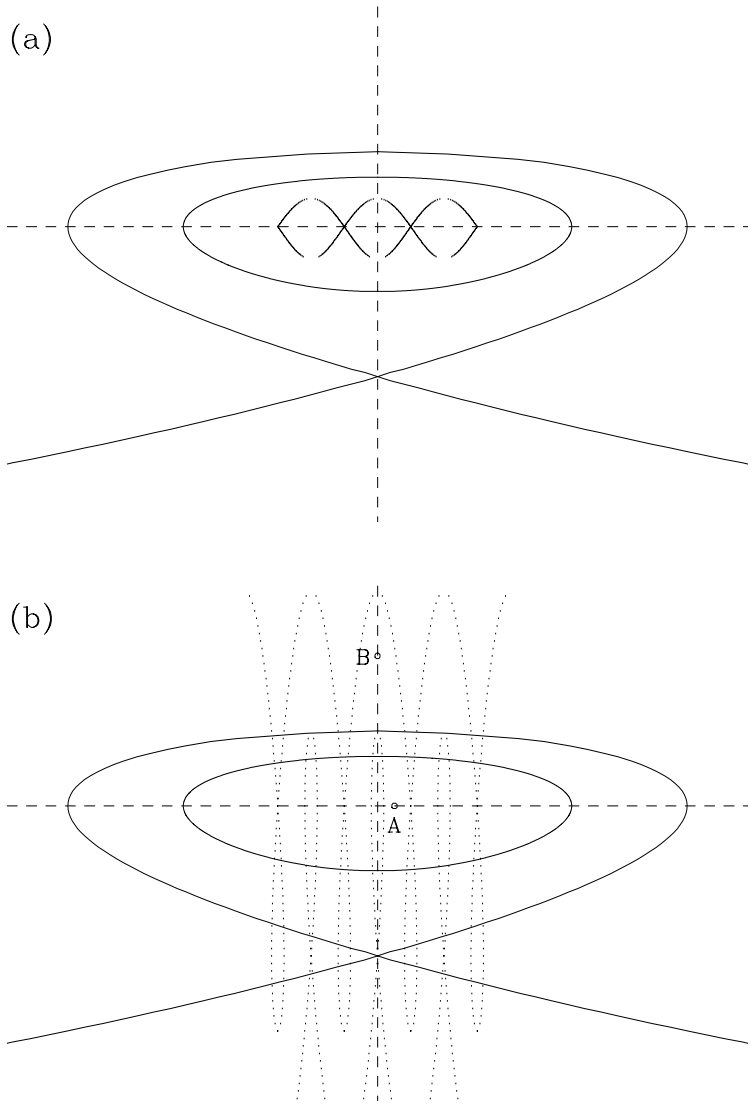

Figure 13: A bunch in a α-like bucket is subjected to self-bunching by a disturbance having a wavelength less than the size of the bunch. The self-bunching buckets are (a) pendulum-like when the coupling impedance is small, and change to (b) α-like when the coupling impedance is large.

This is because the bunch has a momentum spread of $-2\sigma_\delta$ in the negative direction and only $\sim \sigma_\delta$ in the positive direction. The impedance limit becomes

$$\left|\frac{Z_{||}}{n}\right| \lesssim \left(\frac{2\pi|\eta_0|\beta^2 E}{eI_p}\right)\frac{\sigma_\delta^2}{4} \ . \tag{8.9}$$

This amounts to only $|Z_{||}/n| = 0.00055$ Ohm, which is just $\frac{1}{4}$ of the limit in Eq. (8.1). However, if the coupling impedance is large enough, the self-bunching buckets will be α-like instead as depicted in Fig. 13b. This occurs when

$$\left(\frac{6eI_p|Z_{||}/n|}{\pi\beta^2|\eta_0|E}\right)^{1/2} > \left|\frac{\eta_0}{\eta_1}\right| \ , \tag{8.10}$$

according to Eq. (3.2). If we take $|\eta_0/\eta_1| = 3\delta_{\max} = 0.009$, this limit is $|Z_{||}/n| = 0.0066$ Ohm, which is most likely less than the impedance of the vacuum chamber. Note that there are two sets of self-bunching buckets. One set has bucket height from $-|\eta_0/\eta_1|$ to $|\eta_0/2\eta_1|$ and the other from $-|3\eta_0/2\eta_1|$ to 0. Unlike the microwave instability in the usual pendulum-like bucket which may lead only to a growth of longitudinal emittance, here particles will be lost by leaking out from the original α-like bucket of the bunch, while, for example, making synchrotron oscillation inside the self-bunching α-like buckets centered at $\delta = -|\eta_0/\eta_1|$. The rate is just the synchrotron frequency inside the self-bunching bucket or, in terms of number of turns,

$$\Delta N = \frac{1}{2\pi n}\left(\frac{2\pi\beta^2 E}{eI_p|Z_{||}/n||\eta_0|}\right)^{1/2} \ . \tag{8.11}$$

For a broad-band disturbance of $|Z_{||}/n| = 1$ Ohm, centered at 20 GHz or harmonic $n = 5.33\times10^5$, this amounts to $\Delta N = 9.36$ turns.

It is worth pointing out that the self-bunching buckets in Fig. 13 have been sketched over-simplified. The strength of the self-bunching force depends on $I_\ell|Z_{||}|$ where I_ℓ is the local linear current. As we are moving from the center to the edge of the bunch, the self-bunching force will decrease to zero. Therefore, the two series of self-bunching α-like buckets will become fatter away from the bunch center and will eventually merge to form pendulum-like buckets instead near the edge of the bunch.

Bunch particles that are not inside a self-bunching bucket can also be lost. For example, a particle at point A will travel to point B. The time taken can be

computed. Let A be at the point where the phase is $\pi/2$ in unit of the disturbance harmonic and momentum spread zero. From the Hamiltonian (3.1),

$$\Delta N = \frac{\Delta t}{T_0} = \frac{\eta_1^2}{n\eta_0^3}\int_0^{\pi/2}\frac{d\Delta\phi}{p^2+p}\ , \tag{8.12}$$

where

$$p = \frac{\eta_1\delta}{\eta_0} \tag{8.13}$$

is a normalized momentum spread and depends on ϕ through

$$p^3 + \frac{3p^2}{2} = \frac{1}{4} + \frac{3eI_p|Z_{||}/n|}{4\pi\beta^2 E}\frac{\eta_1^2}{\eta_0^3}\cos\Delta\phi\ . \tag{8.14}$$

In Eq. (8.12), T_0 is the revolution period. Therefore, the left side ΔN is the number of turns, and its inverse represents a loss rate, which is proportional to the harmonic n of the disturbance. The integral cannot be performed analytically. However when $I_p|Z_{||}/n|$ is very large, or more exactly when the left side of Eq. (8.14) is very much larger than $\frac{1}{2}$, the integral can be estimated to obtained

$$\frac{1}{\Delta N} = 2n|\eta_0|\left(\frac{3eI_p|Z_{||}/n|}{4\pi\beta^2 E\eta_1}\right)^{2/3}\ . \tag{8.15}$$

With $|\eta_0| = 1\times10^{-6}$, $|\eta_0/\eta_1| = 3\delta_{\max} = 0.009$, and a bunch intensity of 2×10^{12} muons, the integral in Eq. (8.12) is evaluated numerically, and the loss time ΔN is plotted in Fig. 14 for different values of the impedance. Also plotted is the loss rate $1/\Delta N$, which is not far from the dotted curve, which is the estimate given by Eq. (8.15). We see that this loss time is around 1500 turns even when $|Z_{||}/n|$ =1 Ohm, which is very much longer than the 9.36 turn loss time due to synchrotron oscillations inside a self-bunching α-like bucket. Such slow rate may come from the fact that the trajectory AB is situation between two sets of separatrices.

IX. CONCLUSION

In order to have a muon bunch of rms length 3 m and rms momentum spread 0.15% to be stored in the muon collider with a reasonable rf, we found that the slippage factor of the collider must be kept to $|\eta(\delta)| \lesssim 1\times10^{-6}$ for $|\delta| \le \delta_{\max}$.

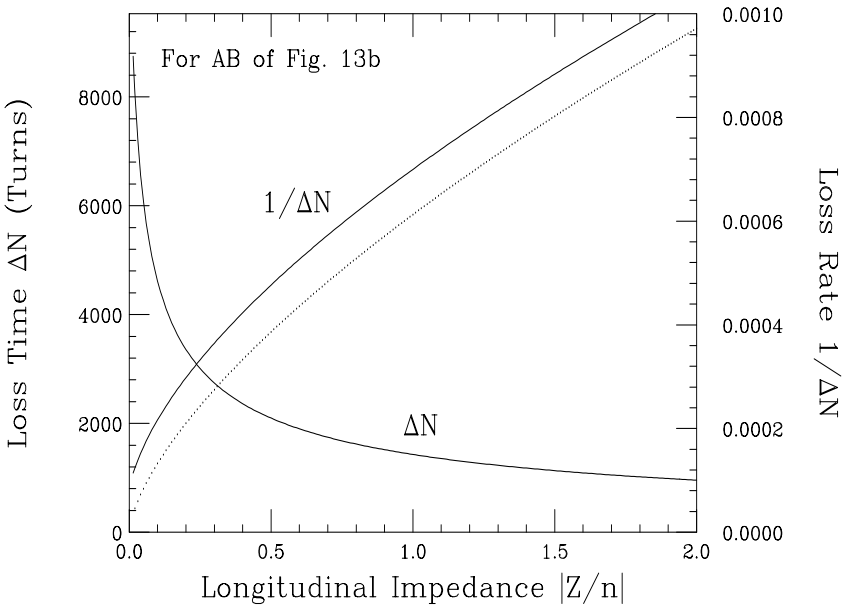

Figure 14: The growth time and growth rate for a bunch inside an α-like bucket, when the self-bunching buckets are also α-like. The dotted curve is an analytic estimate.

In other words, the muon collider must be operating in the quasi-isochronous region.

The zeroth order momentum-compaction factor α_0 of the lattice, and hence the zeroth order slippage factor η_0, can be controlled by adjusting the negative dispersion at the ends of the flexible momentum-compaction module. The first and second orders, α_1 and α_2, or η_1 and η_2, can be controlled by sextupoles. As a result, there are three types of quasi-isochronous buckets. The one dominated by η_0 is the usual pendulum-like bucket. The one dominated by η_0 and η_1 is the α-like bucket. The one dominated by only η_2 is also pendulum like, although there is more nonlinearity. All of these buckets have been discussed. Out of them, the α-like bucket, being asymmetric in momentum spread, is susceptible to longitudinal head-tail instability. Therefore, it is best to eliminate the η_1 contribution through placement of sextupoles.

The lattice will then depend on η_0 and η_2. We found that the η_2 contribution gives rise to large dependency of synchrotron frequency with amplitude. In fact,

if the η_0 contribution is removed, the "potential-well" in the momentum direction is quartic in nature. The synchrotron frequency then starts from zero frequency and rises to a maximum at some amplitude. Such a large variation of synchrotron frequency may be advantageous to damping any mode-coupling instability.

The problem of microwave instability has been investigated. Using the concept of self-bunching, Keil-Schnell criterion for stability has been derived for each of the three quasi-isochronous buckets. We found that the stability limit for the η_0 only bucket is only $|Z_{||}/n| \lesssim 0.0022$ Ohm, and smaller still for the other two buckets. We also argued that it is reasonable to believe the broad-band microwave driving force centered $\gtrsim 15$ GHz, can have a peak value of $|Z_{||}/n| \approx 0.1$ to 1 Ohm. Thus, the growth time can be as short as 12.5 to 39.5 turns. So microwave instability will become the most serious problem of the muon collider.

We also found that in most cases the self-bunch buckets for the muon in the α-like bucket will also be α-like. In that case, particle loss will be inevitable.

We pointed out that the lattice code SYNCH will not be able to compute correctly α_2 although α_1 can be computed rather accurately. Therefore, we must resort to measurement when the lattice is tuned to control α_2.

APPENDIX

The higher orders of the slippage factor must be defined carefully. Here, we follow a derivation of Edwards and Syphers [16]. A particle with momentum offset δ_n sees an *accumulated* rf phase ϕ_n on its n-th passage of the rf cavity, which is considered to have an infinitesimal length. On its $(n+1)$-th passage, at a time $T_{n+1} + \Delta T_{n+1}$ later, the accumulated rf phase seen becomes

$$\phi_{n+1} = \phi_n + \omega_{\rm rf}(T_{n+1} + \Delta T_{n+1}) \ , \tag{A.1}$$

where $\omega_{\rm rf}/2\pi$ is the rf frequency, T_{n+1} is the revolution period of the synchronous particle during its $(n+1)$-th turn and ΔT_{n+1} is the extra time taken by off-momentum particle to complete the revolution. On the other hand, the rf phase seen by the synchronous particle accumulates according to

$$\phi_n^s = \omega_{\rm rf} t_n \ , \tag{A.2}$$

where t_n is the total accumulated time up to the n-th passage of the cavity. Because the off-momentum particle belongs to a bunch with the synchronous particle, we like to measure the rf phase seen relative to the synchronous particle. This leads to the introduction of the rf phase offset or rf phase slip $\Delta\phi_n$ defined by

$$\Delta\phi_n = \phi_n - \phi_n^s = \phi_n - \omega_{\rm rf} t_n \ , \tag{A.3}$$

Substituting into Eq. (A.1) and noting that $T_{n+1} = t_{n+1} - t_n$, we arrive at

$$\Delta\phi_{n+1} = \Delta\phi_n + \omega_{\rm rf}\Delta T_{n+1} \ . \tag{A.4}$$

In order for the synchronous particle to be synchronized, one must adjust the rf frequency so that $\omega_{\rm rf} T_{n+1} = 2\pi h$ for all turns, where h is the rf harmonic number. Now, we can introduce the slippage factor as the slip in revolution period at the $(n+1)$-th passage of the cavity by

$$\frac{\Delta T_{n+1}}{T_{n+1}} = \eta_{n+1}\delta_{n+1} \ . \tag{A.5}$$

Here, the subscript of η implies its dependence on the momentum offset of the particle at the $(n+1)$-th passage and *not* its higher-order expansion term. When smoothing is applied, we obtain the phase-slip equation of Eq. (2.8),

$$\frac{d\Delta\phi}{dt} = \omega_0\eta\delta \ . \tag{A.6}$$

Since the revolution period can be expressed as

$$T = \frac{C}{\beta c} \ , \tag{A.7}$$

we can easily expand T as a Taylor series in δ, from which each higher-order of the slippage factor can be identified. For example, we have

$$\begin{aligned}
\frac{T'}{T_0} &= \frac{C'}{C} - \frac{\beta'}{\beta} \ , \\
\frac{T''}{T_0} &= \frac{2C'^2}{C^2} - \frac{2\beta' C'}{\beta C} - \frac{\beta''}{\beta} + \frac{2\beta'^2}{\beta^2} \ , \\
\frac{T'''}{T_0} &= \frac{C'''}{C} - \frac{3\beta' C''}{\beta C} - \frac{3\beta'' C'}{\beta C} + \frac{6\beta'^2 C'}{\beta^2 C} - \frac{\beta'''}{\beta} - \frac{\beta'\beta''}{\beta^2} - \frac{6\beta'^3}{\beta^3} \ ,
\end{aligned} \tag{A.8}$$

where the *prime* denotes differentiation with respect to δ and all variables are evaluated at the synchronous values, i.e., with subscript zero. The derivatives of C can be read off easily from Eq. (2.7). The derivatives of β can be computed straightforwardly. They are:

$$\begin{aligned}
\frac{\beta'}{\beta} &= \frac{1}{\gamma^2} \ , \\
\frac{\beta''}{\beta} &= -\frac{3\beta^2}{\gamma^2} \ , \\
\frac{\beta'''}{\beta} &= -\frac{3\beta^2(1-5\beta^2)}{\gamma^2} \ .
\end{aligned} \tag{A.9}$$

With the expansion of the slippage factor

$$\eta = \eta_0 + \eta_1\delta + \eta_2\delta^2 + \cdots \ , \tag{A.10}$$

the expressions for η_0, η_1, and η_2 in Eqs. (2.10), (2.11), and (2.10) are obtained.

Looking at the phase slip equation above, one may be tempted to relate $d\Delta\phi/dt$ to $-\Delta\omega/h$. This will translate the equation to

$$\frac{\Delta\omega}{\omega_0} = -\eta\delta \ . \tag{A.11}$$

which is different from Eq. (A.5) and therefore lead to incorrect expressions for the higher-order terms of η. This misconception comes about in the smoothing procedure from Eq. (A.4) to Eq. (A.6), where we divide throughout by the *synchronous* period. If $\Delta\omega$ of the off-momentum particle is desired, one should

divide instead by $T_{n+1} + \Delta T_{n+1}$, the revolution period of the off-momentum particle.

Another definition in the literature is [17]

$$\eta = -\frac{1}{\omega_0}\frac{d\omega}{d\delta} \ , \tag{A.12}$$

which is incompatible with the phase-slip equation in Eq. (A.6). This definition originates from the lowest expansion in ω [18], and is therefore insufficient when higher-orders in η are studied. This is, in fact, a variation of the incorrect definition of Eq. (A.11).

References

[1] S.Y. Lee, K.Y. Ng, and D. Trbojevic, Phys. Rev.E, **48**, 3040-3048 (1993).

[2] A. Garren, et al., *Design of the Muon Collider Lattice: Present Status*, to appear in Proc. San Francisco Workshop Physics of Muon Colliders, 1996.

[3] C. Johnstone, K.Y. Ng, and D. Trbojevic, *Interaction Regions with Increased Low-Betas for a 2-TeV Muon Collider*, Proc. 9th Advanced ICFA Beam Dynamics Workshop on Beam Dynamics and Technology Issues for $\mu^+\mu^-$ Colliders, Montauk, NY, Oct. 15-20, 1995, ed. J. Gallardo, p.178.

[4] D. Boussard and T. Linnecar, Proc. 2nd European Particle Accelerator Conference, Nice, June 990, Ed. P. Martin and P. Mandrillon, p. 1560.

[5] A. Riabko, M. Bai, B. Brabson, C.M. Chu, X. Kang, D. Jeon, S.Y. Lee, and X. Zaho, *Particle Dynamics in Quasi-Isochronous Storage Rings*, to be published in Phys. Rev. E, 1996.

[6] K. Ng, *Higher-order Momentum Compaction for a Simplified FODO Lattice and Comparison with SYNCH,* Fermilab Report FN-578, 1991.

[7] The $\mu^+\mu^-$ Collider Collaboration, *Muon Muon Collider: A Feasibility Study*, 1996, Ed. J. Gallardo, p.326. Also published as Internal Lab. Notes: BNL-52503, Fermi Lab-Conf.-96/092, and LBNL-38946.

[8] C. Johnstone, private communication.

[9] A.A. Garren, A.S. Kenney, E.D. Courant, and M.J. Syphers, *A User's Guide to SYNCH*, Fermilab Internal Note FN-420, 1985.

[10] D. Robin, H. Hama, and A. Nadji, *Experimental Results on Low Alpha Electron-Storage Rings*, Proc. Micro Bunches Workshop, Upton, NY, Sep. 28-30, 1995, Ed. E.B. Blum, M. Dienes, and J.B. Murphy, (AIP Conf. Proc. 367), p. 150; D. Robin, R. Alvis, A. Jackson, R. Holtzapple, and B. Podobedov, '*Low Alpha Experiments at the ALS*, *ibib* p. 181.

[11] H. Hama, S. Takano, and G. Isoyama, Nucl. Inst. Meth. **A329**, 29 (1993).

[12] S. Krinsky and J.M. Wang, Part. Accel. **17**, 109 (1985).

[13] H. Henke, *Point Charge Passing a Resonator with Beam Tubes*, CERN Report CERN-LEP-RF/85-41.

[14] Figures 11 and 12 are produced from a formula with is valid when $g/b \ll 1$. This formula is very much simpler than the original one derived by Henke. See for example, K.Y. Ng, *Impedances of Bellows Corrugations*, Proc. IEEE Part. Accel. Conf., March 16-19, 1987, Washington, DC, Ed. E.R. Lindstrom and L.S. Taylor, p.1051.

[15] K.Y. Ng, *Impedances of the Shielded Bellows in the SSC and the Effects on Beam Stability*, Report of the SSC Impedance Workshop, June 26-27, 1985, SSC-SR-1017, p. 61.

[16] D.A. Edwards and M.J. Syphers, *An Introduction to the Physics of High Energy Accelerators*, Wiley and Sons, 1993.

[17] J. Wei, *Longitudinal Dynamics of the Non-Adiabatic Regime on Alternating-Gradient Synchrotrons*, PhD Dissertation, SUNY, Stony Brook, 1990.

[18] See for example, E.D. Courant, R. Ruth, W. Weng, L. Michelotti, D. Neuffer, and L. Teng, AIP Conf. Proc. No. 87, 36 (1982).